Philosophical Magazine. Vol. 86. Núm. 15. 2006. Pag. 2271-2282
http://dx.doi.org/10.1080/14786430500300074

Ball milling nanocrystallization of arc-melted and melt-spun $Fe_{78}Co_5Nb_3Zr_3B_5Ge_5Cu_1$ alloy: Microstructure and magnetic properties

J. S. BLÁZQUEZ †, V. FRANCO †, A. CONDE †*, S. ROTH ‡

† *Departamento de Física de la Materia Condensada. ICMSE-CSIC. Universidad de Sevilla. P.O. Box 1065. 41080 Sevilla, Spain.*

‡ *IFW-Dresden, Institute for Metallic Materials, Helmholtzstrasse 20, 01069 Dresden, Germany.*

The viability of developing a nanocrystalline microstructure for the $Fe_{78}Co_5Nb_3Zr_3B_5Ge_5Cu_1$ composition using a planetary ball mill was studied. Two starting samples were chosen: an arc-melted ingot and a partially crystallized melt-spun ribbon. The α-Fe phase was detected in both initial samples, although different intermetallic phases were detected in each of them. Milling at 150 rpm, these intermetallics disappeared after 5 h for the melt-spun alloy (*RQ*) and did not disappear even after 70 h for the arc-melted sample (*AM*). However, the α-Fe phase became nanosized in both cases. A good thermal stability was found for the *RQ* alloy after 10 hours of milling, although the nanocrystal size increased from ~8 to ~20 nm after heating up to 973 K. The *AM* samples exhibited a lower coercivity and a higher magnetization than *RQ* samples.

Keywords: Nanocrystalline Materials; Mechanical Alloying; Magnetic Properties.

*Corresponding author: Prof. A. Conde
Departamento de Física de la Materia Condensada. Universidad de Sevilla.
Apartado 1065, 41080 Sevilla (Spain).
Phone: (34) 95 455 28 85
Fax: (34) 95 461 20 97
E-mail: conde@us.es

Philosophical Magazine. Vol. 86. Núm. 15. 2006. Pag. 2271-2282
http://dx.doi.org/10.1080/14786430500300074

1. Introduction

Soft magnetic nanocrystalline alloys with a microstructure consisting of nano-sized α-Fe type crystallites embedded in a residual amorphous matrix are among the softest magnetic materials known up to date [1]. Generally, the microstructure of these alloys is achieved in a procedure consisting of two steps: first, an amorphous alloy is obtained with the desired composition and, afterwards, this precursor is conveniently annealed to develop a nanocrystalline microstructure. In order to obtain an amorphous alloy by quenching a melted system with a suitable composition to develop a nanocrystalline microstructure, it is necessary to use very high quenching rates (~10^5-10^6 K/s). These very high cooling rates limit the geometry of the material to films or ribbons with a maximum thickness of few tens of microns. In order to overcome this limitation, consolidation of metallic powders has been proposed as a suitable technique to produce bulk shaped materials [2], widening their possible technological applications. In this sense, mechanical milling has been shown as an advantageous procedure to obtain nanocrystalline powder in many different composition systems [3,4]. However, the coercivity of the consolidated powder is 2-3 orders of magnitude larger than the values observed in melt-spun nanocrystalline ribbons, which has been associated to the absence of a residual amorphous matrix in the case of the mechanically milled nanocrystalline samples [2]. Therefore, the distribution of the atoms out of the α-Fe nanocrystals, forming intermetallics or segregated at the grain boundaries and its thermal stability are interesting subjects to study.

In this work, the preparation of a nanocrystalline $Fe_{78}Co_5Nb_3Zr_3B_5Ge_5Cu_1$ alloy by milling has been studied. The addition of Ge and Co to Fe-based nanocrystalline alloys has been proposed in order to enhance the magnetic properties of the system at

Philosophical Magazine. Vol. 86. Núm. 15. 2006. Pag. 2271-2282
http://dx.doi.org/10.1080/14786430500300074

high temperatures [5-7]. There are a lot of parameters influencing the milling process for a given composition: type of mill, time, speed and media of milling, ball-to-powder ratio, starting material, etc. This study is devoted to the dependency of the milling process on the microstructure of the starting system for the same composition and, therefore, the other milling variables were kept constant. Two initial samples were chosen: an arc-melted ingot and a partially crystallized ribbon obtained by melt-spinning. Both systems are compositionally homogeneous at the scale of the powder particles (~μm). This fact implies several advantages in comparison with the use of elemental powders as starting materials, especially in such complex compositions as the one studied in this work. The milling of elemental powders would need much more time to homogenize the composition and it would be quite hard to assure that the final composition will remain as the initial proportion of powder used due to preferential sticking of some elements on the milling media. On the other hand, a homogeneous composition is less reactive than pure elements, which will reduce the effect of oxygen contamination in the powder.

2. Experimental

A master alloy with the nominal composition $Fe_{78}Co_5Nb_3Zr_3B_5Ge_5Cu_1$ was obtained by arc-melting several times in an argon atmosphere and after purifying the atmosphere by melting titanium (*AM* sample). A portion of this alloy was melted again and rapidly quenched by using a single-roller Bühler melt-spinner (*RQ* sample). The ball milling was performed under argon atmosphere in a Retsch PM4000 planetary ball mill using hardened steel balls and bowls. The rotation speed was 150 rpm for all the experiments and the ball to powder ratio was 10:1.

Philosophical Magazine. Vol. 86. Núm. 15. 2006. Pag. 2271-2282
http://dx.doi.org/10.1080/14786430500300074

The *RQ* ribbon, ~100 μm thick, was very brittle and thus, it was easy to make flakes which were used as the starting material for the milling procedure. After 2 h of milling, these flakes are still present and thus it is not possible to consider this *RQ* sample as a real powder at this stage.

In order to obtain pieces of the *AM* sample small enough to start the milling in the planetary mill, big pieces (several mm) were pulverized using a SPEX shaker mill for short times (< 0.5 h). The XRD pattern of the obtained *AM* powder after milling in the SPEX did not show significant differences to the bulk *AM* alloy, except for a broadening of the diffraction maxima.

The thermal stability of the samples was studied by annealing the powder in an argon atmosphere, using a differential scanning calorimeter (DSC) Netzsch DSC 404. The melting interval of the studied composition starts about $T_m \sim 1450$ K, as shown in Figure 1. The microstructure of the different samples was studied using a Philips PW 1050 diffractometer with Co Kα radiation. Room temperature magnetic properties of the samples were characterized using a vibrating sample magnetometer (VSM) for the saturation magnetization, M_S, and a Förster Koerzimat for the coercivity, H_C. The morphology of the powder was studied with a scanning electron microscope (SEM) Philips XL-30 using secondary electrons mode.

'[Insert figure 1 around here]'

Some of the resultant powder was pressed at 973 K ~ $(2/3)T_m$ during 5 min in vacuum, applying 575 MPa in an uniaxial hot press, in order to obtain bulk disk-shaped samples of 10 mm diameter and several mm high. The consolidation was also possible at 773 K ~ $(1/2)T_m$ in the same conditions but unsuccessful at 573 K ~ $(2/5)T_m$. These bulk samples were prepared to check the reliability of the coercivity results obtained for powder samples using the Koerzimat.

Philosophical Magazine. Vol. 86. Núm. 15. 2006. Pag. 2271-2282
http://dx.doi.org/10.1080/14786430500300074

3. Results and discussions

3.1 Microstructure

Figures 2 and 3 show the XRD patterns of the *RQ* and *AM* samples after different times of milling. In the case of the *AM* sample labelled as-cast, the XRD pattern corresponds to the arc-melted ingot and, in the case of the *RQ* sample, it corresponds to the melt-spun ribbon. As it can be observed for both as-cast samples XRD patterns present α-Fe crystalline peaks but also other diffraction maxima of some crystalline phases can be detected. The XRD patterns of the *RQ* samples show peaks corresponding to metastable phase(s), which become negligible after 5 h of milling. However, the diffraction maxima of the *AM* samples can be indexed using the peaks of NbFeB and Fe_2Zr phases. Unlike for *RQ* samples, these peaks do not disappear even after 70 h of milling. A tentative explanation of this fact must take into account the lower cooling rate of the melted composition in the case of the *AM* samples in comparison with that of the *RQ* samples. This provokes that the formation of stable crystalline phases different to α-Fe is overcome in the case of the initial *RQ* ribbon (quenching rate of $\sim 10^5$-10^6 Ks^{-1}), although some metastable crystalline phases appear. The metastability of these phases could be the responsible of the easiness for destroying them during milling, while the energy supplied by milling during our experiments was not enough to destroy the thermodynamically stable phases (α-Fe, NbFeB or Fe_2Zr in the initial *AM* sample).

'[Insert figures 2 and 3 around here]'

The evolution of the α-Fe phase with the milling time and the thermal treatment was studied for both sets of samples after fitting the XRD profile in the 2θ range

Philosophical Magazine. Vol. 86. Núm. 15. 2006. Pag. 2271-2282
http://dx.doi.org/10.1080/14786430500300074

between ~40-60 degrees. The main contribution corresponds to the (110) diffraction maximum of α-Fe, fitted as a Pseudovoigt function. For a short milling time, tiny crystalline peaks of intermetallic phases appear in this 2θ range (fitted as Lorentzian functions for simplification). In the case of *RQ* samples, an amorphous halo (simulated as a Gaussian peak) was also necessary to fit the XRD profile. In the case of the *AM* samples, the Lorentzian contribution to the Pseudovoigt function increases from 0.3 up to 0.6 with the milling time and, after heating up to 973 K, decreases to 0.3, independently of the milling time. This indicates that the relative effect of the small grain size on the broadening of the diffraction maxima increases with the milling time in comparison with the microstrain contribution and decreases with the annealing process. In the case of the *RQ* samples, the Lorentzian contribution is higher (decreasing from ~1 to 0.7 as the milling time increases, being ~1 after annealing). This indicates that the effect on the broadening of the (110) maximum for the *RQ* samples due to microstrain relative to small crystal size increases with the milling time, unlike for *AM* samples. From the broadening of the (110) deconvoluted maximum, it was possible to estimate the grain size, $<D>$, and the microstrain, ε. On the other hand, the lattice parameter was measured using the (110) and (200) diffraction maxima of the α-Fe phase. These results appear in table 1.

'[Insert table 1 around here]'

As it is expected, the microstrain of the samples increases with the milling time for both *RQ* and *AM* systems from 0.006 up to 0.020 (after 15 h of milling) and up to 0.008 (after 70 h of milling), respectively. This indicates a more significant and much faster increase of the microstrain for *RQ* samples than for *AM* samples. After annealing, the microstrain of the *RQ* samples could not be measured due to the negligible Gaussian

Philosophical Magazine. Vol. 86. Núm. 15. 2006. Pag. 2271-2282
http://dx.doi.org/10.1080/14786430500300074

contribution to the broadening of the (110) diffraction maximum, whereas *AM* samples do not show significant change.

The decrease in grain size of the α-Fe phase saturates in both types of samples at 8 nm, which is in good agreement with the value observed for pure Fe [8]. However, this value is obtained after 5 h of milling for the *RQ* alloy and only after 50 h of milling for the *AM* alloy. On the other hand, only the *RQ* samples milled during 10 and 15 h and heated up to 975 K remain with a value of *D* below 20 nm. For *AM* samples, the annealing process increases the grain size to 20 nm or higher, even for milling times of 70 h. This fact indicates that a certain microstructural stability can be achieved for the *RQ* sample after 10 h of milling but the microstructure of the *AM* samples is less thermally stable even after 70 h of milling. In fact, experiments performed on *RQ* sample heated up to 573 K show that the nanocrystal size increases from 8 to 15 nm for the alloy milled during 5 h, but the samples milled 10 and 15 h show the same crystal size after that thermal treatment. Figure 4 shows the XRD pattern of those *RQ* samples heated up to 973 K, for which α-Fe was the only crystalline phase detected after milling.

'[Insert figure 4 around here]'

The lattice parameter, *a*, does not differ for both as-cast samples (0.2874 and 0.2873 nm for the *RQ* and the *AM* alloys, respectively), but presents a different evolution during the milling and annealing processes. In the case of *RQ* samples, *a* is almost constant throughout the milling process and after annealing the sample. However, for *AM* samples, the lattice parameter increases for long milling times up to 0.2884 nm and a clear reduction of *a* down to ~0.2860 nm is detected after annealing, even for samples milled during short times. Figure 5 shows the *a* values as a function of

Philosophical Magazine. Vol. 86. Núm. 15. 2006. Pag. 2271-2282
http://dx.doi.org/10.1080/14786430500300074

the milling time for both set of samples. The value of pure α-Fe phase is also shown for comparison.

'[Insert figure 5 around here]'

The constant value of *a* for *RQ* samples is clearly larger than that of pure α-Fe (0.28663 nm) indicating the presence of some stable impurities in the crystal lattice. Although long milling time of *AM* samples yields an increase of the lattice parameter of the α-Fe phase, it is worth noting that *RQ* samples were not submitted to such long milling times and, therefore, this increase could be ascribed to the higher energy accumulated for *AM* samples.

The decrease of *a* observed after annealing *AM* samples occurs even for short milling times, comparable to those of *RQ* samples, for which no change in *a* is detected. This fact might be ascribed to the presence of stable intermetallic phases in the *AM* samples unlike for the *RQ* samples. The elements of the studied composition with better solubility in the α-Fe phase are Co and Ge. Although Co is highly soluble in α-Fe [9], the solubility of Ge is much more reduced (up to 10 at % at room temperature) [9]. The mixing enthalpies of Ge with Nb and Zr (-24 and -25 kJ/mol, respectively) are much lower than those of Fe with the two other elements (-3 and -1 kJ/mol, for Nb and Zr respectively) [10]. Therefore, it is possible that during annealing Ge atoms diffuse to the intermetallics, rich in Nb and Zr, and thus the α-Fe phase will reduce the concentration of this element, in agreement with the reduction of *a* observed for annealed *AM* samples. The value of *a* observed for *RQ* samples and not annealed *AM* samples after low milling times, ~0.2873 nm, would correspond to a Ge content of 4 at % [11], as Co does not influence the lattice parameter of α-Fe below 10 at % and for higher content *a* decreases [12]. The other elements Nb, Zr and B are strongly insoluble in the α-Fe phase. For *AM* samples, these elements might be found preferentially in the

Philosophical Magazine. Vol. 86. Núm. 15. 2006. Pag. 2271-2282
http://dx.doi.org/10.1080/14786430500300074

intermetallics; however, in the case of *RQ* samples, the boundaries between nanocrystals are suitable regions to be enriched in these elements.

3.2 Magnetic properties

In order to perform magnetic measurements, the powder samples were encapsulated in silver foil, which was folded in order to avoid the movement of the powder inside. Saturation magnetization, M_S, was measured in the VSM (the maximum applied field was 1500 kA/m) and the Koerzimat was used to obtain a value of coercivity, H_C, after magnetizing the sample with an applied field of 200 kA/m. The resultant values appear in table 2.

'[Insert table 2 around here]'

It is worth noting that these values of H_C were obtained in such a system consisting of a mixture of powder and air gaps. However, considering the repetitiveness of the measurement (low errors bar) and that all the samples were prepared in the same way, the reported values could be considered as self-comparable under this study. On the other hand, the *RQ* powder milled during 15 h and the *AM* powder milled during 70 h were pressed at 973 K during 5 min in order to form bulk disks (1 cm in diameter and several mm high) and the coercivity measured in these two bulk samples is in good agreement with those of the corresponding powder samples encapsulated in silver and heated up to 973 K (see table 2). Once this consideration is established, it is possible to observe lower values of coercivity for the *AM* samples than for the *RQ* samples, about 2500-3000 and 4500-5000 A/m, respectively. In both cases, annealing of the samples reduces the value of H_C. Figure 6 shows the H_C values for the different studied samples.

Philosophical Magazine. Vol. 86. Núm. 15. 2006. Pag. 2271-2282
http://dx.doi.org/10.1080/14786430500300074

It is worth noting that *RQ* sample milled during 2 h is not a real powder sample but consist of ribbon flakes. Therefore, this sample was discarded for the annealing.

'[Insert figure 6 around here]'

The M_S values do not significantly change with the milling time or the annealing process. Although average values observed for *AM* samples (~170 emu/g) are higher than those of the *RQ* samples (~160 emu/g), these variations are close to the error bar and a dependency cannot be clearly established.

The decrease of the coercivity with the annealing process for the two studied types of samples could be due to a relaxation of the internal stresses of the particles. However, the different absolute values for *RQ* and *AM* samples (both encapsulated powder and pressed bulk disks) is not easy to interpret due to the large number of parameters which define the system: micrometric powder composed of nanocrystalline α-Fe plus other crystalline phases (NbFeB and Fe_2Zr) in the case of the *AM* system.

It is worth noting that the trend of H_C is not consistent with the evolution of the nanocrystal size in the frame of Herzer's model [13]. In fact, samples with the same value of *D* show very different H_C values: e.g. *RQ* samples after 5, 10 and 15 h of milling and *AM* samples after 50 and 70 h of milling (see tables 1 and 2). On the other hand, after annealing, an increase of *D* is observed but a decrease of H_C is measured. Therefore, the averaging out of magnetocrystalline anisotropy due to the very fine microstructure predicted by Herzer's model is not the main fact describing the evolution of the coercivity of the powder samples studied in this work and other explanation is required.

The evolution of the size of the powder particles might affect the coercivity of the system. Images of the powders obtained by SEM show that for both *RQ* and *AM* samples, the maximum of the particle size distribution saturates at ~25 μm as milling

Philosophical Magazine. Vol. 86. Núm. 15. 2006. Pag. 2271-2282
http://dx.doi.org/10.1080/14786430500300074

time increases. For all the samples, the smaller particles are ~5 μm in size. Two characteristic SEM images are given in Fig. 7, corresponding to *RQ* sample milled for 10 h and *AM* sample milled for 50 h. The latter shows a more homogeneous particle size, related to the longer milling time. Therefore, the monotonous evolution of particle size is not sufficient to explain the observed behaviour of coercivity, which is not monotonous (see Fig. 6). Moreover, the differences in coercivity between the two sets of samples can not be explained either by the different particle size of the powder: a higher coercivity is obtained for *RQ* samples, which have bigger particles.

'[Insert figure 7 around here]'

On the other hand, coercivity might be affected by the magnetoelastic contribution to the anisotropy. In fact, this could explain the differences observed between the two set of samples. *AM* samples exhibit a lower microstrain than *RQ* samples, which could yield lower magnetoelastic anisotropy for similar values of magnetostriction. Besides, the presence of several magnetic phases in the *AM* system could reduce the magnetostriction of the whole system by averaging if the signs of the contributions of the different magnetic phases are opposite: the magnetostriction of Fe_2Zr is -11 ppm [14] and, although the value of magnetostriction for pure α-Fe is -9 ppm it becomes positive for small Co content [15].

On the other hand, the disappearance of intermetallics (rich in Zr, Nb and B) after milling *RQ* samples implies that the nanocrystal boundaries may be enriched in Zr, Nb and B, non-magnetic atoms insoluble in the α-Fe phase. The effect of a nanocrystal boundary enriched in these atoms, as it might occur in *RQ* samples, could provoke a more deleterious effect on the magnetic properties through an impingement of the exchange coupling between nanocrystals [16] than that produced by the presence of intermetallic inclusions in *AM* samples through domain wall pinning.

Philosophical Magazine. Vol. 86. Núm. 15. 2006. Pag. 2271-2282
http://dx.doi.org/10.1080/14786430500300074

4 Conclusions

A nanocrystalline microstructure has been developed for the $Fe_{78}Co_5Nb_3Zr_3B_5Ge_5Cu_1$ composition using a planetary ball mill. An α-Fe phase was detected in both arc-melted ingot and partially crystallized melt-spun ribbon (*AM* and *RQ* samples, respectively) in their initial state, although different intermetallic phases were detected in each of them: Fe_2Zr and NbFeB stable intermetallic phases in the case of *AM* sample, and unidentified metastable phase(s) in the case of *RQ* sample. These intermetallics disappeared after 5 h of milling at 150 rpm for the *RQ* sample and did not disappear even after 70 h of milling for the *AM* sample. However, the α-Fe phase became nanosized in both cases.

A good thermal stability was found for the melt-spun alloy after 10 hours of milling, with a negligible microstructural change after heating up to 573 K, although the nanocrystal size increases from ~8 to ~20 nm in samples heated up to 973 K.

Magnetic properties show that, after milling, the *AM* sample is softer than the *RQ* sample, even for consolidated bulk samples. The softer values observed for the *AM* samples could be due to a reduction of the magnetoelastic anisotropy and/or to a more deleterious effect on the magnetic properties due to an impingement of the exchange coupling between nanocrystals by a nanocrystal boundary enriched on Zr, Nb and B, in the case of *RQ* samples, than the domain pinning effect due to the presence of intermetallics in *AM* samples.

Acknowledgements

This work was supported by the Spanish Government and EU FEDER (Project MAT 2004-04618). J.S. Blázquez acknowledges a research contract from the Regional Government of Andalucía (Spain).

Philosophical Magazine. Vol. 86. Núm. 15. 2006. Pag. 2271-2282
http://dx.doi.org/10.1080/14786430500300074

References

[1] McHenry ME, Willard MA, Laughlin DE, Prog Mater Sci 44 (1999) 291.

[2] R. Gupta, S. Enzo, R. Frattini, A. Hernando, P. Marín, G. Mulas, A. Perin, G. Principi, J Non-Equilibrium Proc, 10 (1998) 283.

[3] C. Suryanarayana, Prog Mater Sci 46 (2001) 1.

[4] D. L. Zhang, Prog Mater Sci 49 (2004) 537.

[5] M. A. Willard, D. E. Laughlin, M. E. McHenry, D. Thoma, K. Sickafus, J. O. Cross, J Appl Phys 84 (1998) 6773.

[6] K. Suzuki, J. W. Cochrane, J. M. Cadogan, X. Y. Xiong, K. Hono, J Appl Phys 91 (2002) 8417.

[7] J. S. Blázquez, S. Roth, C. Mickel, A. Conde, Acta Mater 53 (2005) 1241.

[8] C. C. Koch, Nanostruct Mater 9 (1997) 13.

[9] T. B. Massalski, H. Okamoto, P.R. Subramanian, L. Kacprzak. Binary alloys phase diagrams. Materials Park (OH): ASM International; 1992. p. 1187, 1706.

[10] F. R. de Boer, R. Boom, W. C. M. Mattens, A. R. Miedema, A. K. Niessen. Cohesion in metals. Transition metal alloys. Amsterdam: North-Holland; 1989. p.

[11] W. B. Pearson. A handbook of lattice spacings and structures of metals and alloys, vol. 2. Oxford: Pergamon Press; 1967. p. 911.

[12] R. M. Bozorth. Ferromagnetism. Princeton (NJ): Van Nostrand; 1968. p. 192.

[13] G. Herzer, IEEE Trans. Magn. 25 (1989) 3327.

[14] G. Concas, F. Congiu, G. Spano, M. Bionducci, J Magn Magn Mater 279 (2004) 421.

[15] R. C. O'Handley. Modern magnetic materials: principles and applications. New York: Wiley; 1999. p. 227.

[16] A. Hernando, M. Vázquez, T. Kulik, C. Prados, Phys. Rev. B 51 (1995) 3581.

Philosophical Magazine. Vol. 86. Núm. 15. 2006. Pag. 2271-2282
http://dx.doi.org/10.1080/14786430500300074

Table 1. Microstructural parameters

Initial alloy	miling time (h)	As-milled		Heated up to 973 K	
		$a \pm 0.0005$ (nm)	$D \pm 5$ (nm)	$a \pm 0.0005$ (nm)	$D \pm 5$ (nm)
Melt-spun ribbon (*RQ*)	0	0.2874	28	*	*
	2	0.2873	16	*	*
	5	0.2870	8	0.2872	22
	10	0.2876	9	0.2872	17
	15	0.2876	8	0.2873	17
Arc-melted master alloy (*AM*)	0	0.2873	21	0.2859	**
	10	0.2873	14	0.2852	**
	20	0.2871	11	0.2861	**
	30	0.2871	10	0.2865	27
	50	0.2881	8	0.2864	21
	70	0.2884	8	0.2860	20

* Measurements performed on melt-spun ribbon (0 h) or ribbon flakes (2 h). Not real powder and, therefore, excluded for the annealing study.

** The grain size is too big to be measured from the broadening of the diffraction maximum.

Philosophical Magazine. Vol. 86. Núm. 15. 2006. Pag. 2271-2282
http://dx.doi.org/10.1080/14786430500300074

Table 2. Magnetic parameters

Initial alloy	miling time (h)	As-milled		Heated up to 973 K	
		H_C (A/m)	$M_S \pm 5$ (emu/g)	H_C (A/m)	$M_S \pm 5$ (emu/g)
Melt-spun ribbon (*RQ*)	0	(*) 2933 ± 14		**	**
	2	4800 ± 700	160	**	**
	5	4980 ± 70	159	4545 ± 180	159
	10	4930 ± 140	161	4328 ± 20	162
	15	4300 ± 30	159	3860 ± 220	163
Compacted *RQ* sample at 973 K	15			3860 ± 30	
Arc-melted master alloy (*AM*)	0	2630 ± 110	169	1960 ± 100	162
	10	2880 ± 40	168	2170 ± 20	163
	20	3230 ± 60	172	2550 ± 80	170
	30	3030 ± 60	169	2540 ± 60	174
	50	2960 ± 40	171	2740 ± 10	173
	70	2630 ± 20	170	2410 ± 20	172
Compacted *AM* sample at 973 K	70			2390 ± 50	

* Measurements performed on a single piece of the melt-spun ribbon.

** Measurements performed ribbon flakes. Not real powder and, therefore, excluded for the annealing study.

Philosophical Magazine. Vol. 86. Núm. 15. 2006. Pag. 2271-2282
http://dx.doi.org/10.1080/14786430500300074

Figure captions

Figure 1. DSC scans at 20 K/min showing the melting and solidifying behaviour of the composition $Fe_{78}Co_5Nb_3Zr_3B_5Ge_5Cu_1$.

Figure 2. XRD patterns of powder obtained from a melt-spun ribbon after milling for different times.

Figure 3. XRD patterns of powder obtained from an arc-melted alloy after milling for different times.

Figure 4. Room temperature XRD patterns of *RQ* samples annealed at 973 K.

Figure 5. Lattice parameter, *a*, as a function of the milling time for both *RQ* and AM samples in the as-milled and annealed state.

Figure 6. Coercivity, H_C, as a function of the milling time for both *RQ* and *AM* samples in the as-milled and annealed state.

Figure 7. Secondary electrons SEM images of *AM* sample milled for 50 h (upper) and *RQ* sample milled for 10 h (lower). The bar corresponds to 100 μm.

Philosophical Magazine. Vol. 86. Núm. 15. 2006. Pag. 2271-2282
http://dx.doi.org/10.1080/14786430500300074

Figure 1

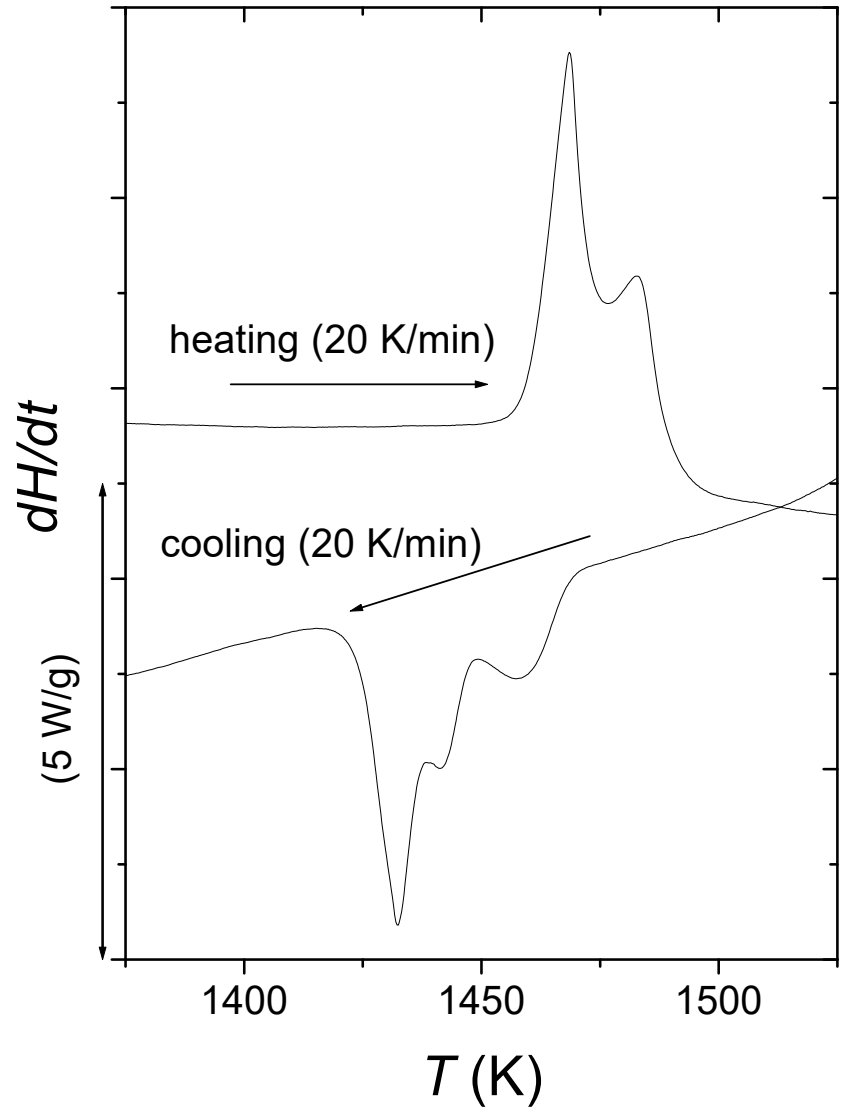

Philosophical Magazine. Vol. 86. Núm. 15. 2006. Pag. 2271-2282
http://dx.doi.org/10.1080/14786430500300074

Figure 2

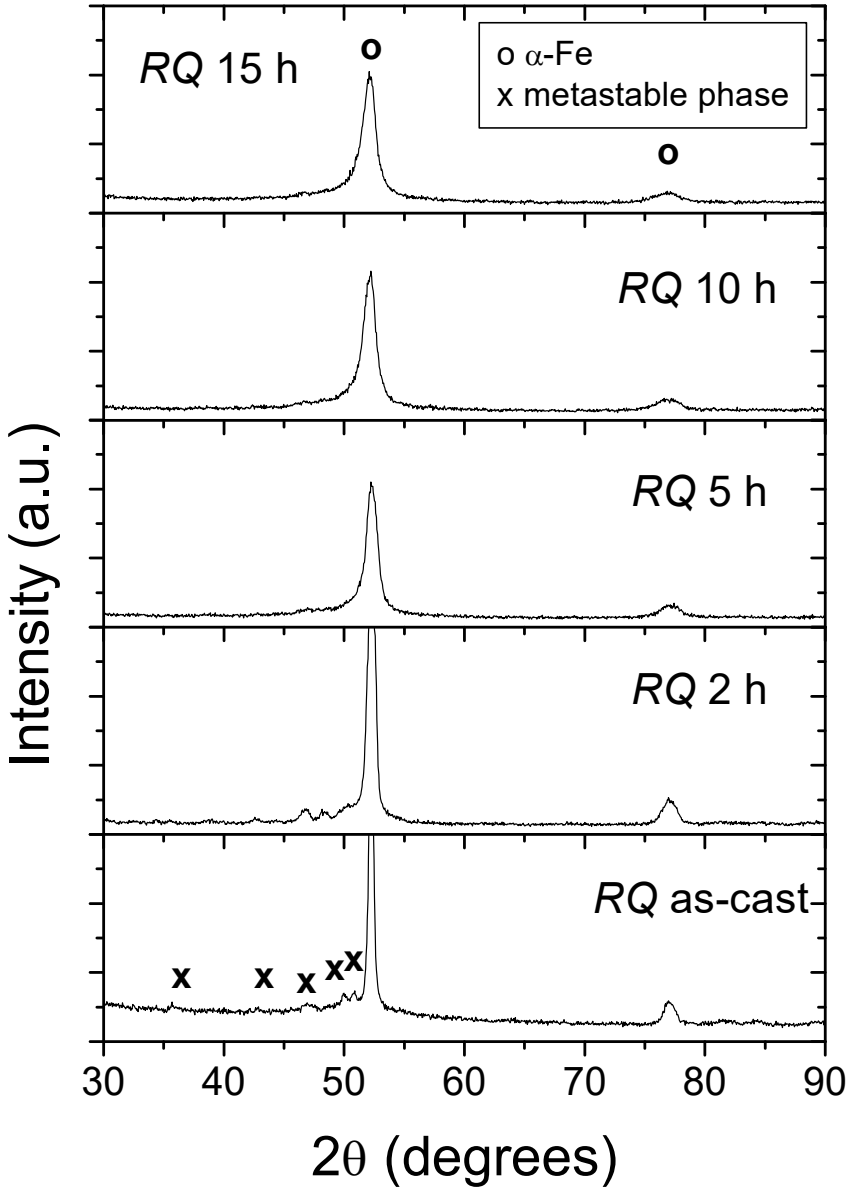

Philosophical Magazine. Vol. 86. Núm. 15. 2006. Pag. 2271-2282
http://dx.doi.org/10.1080/14786430500300074

Figure 3

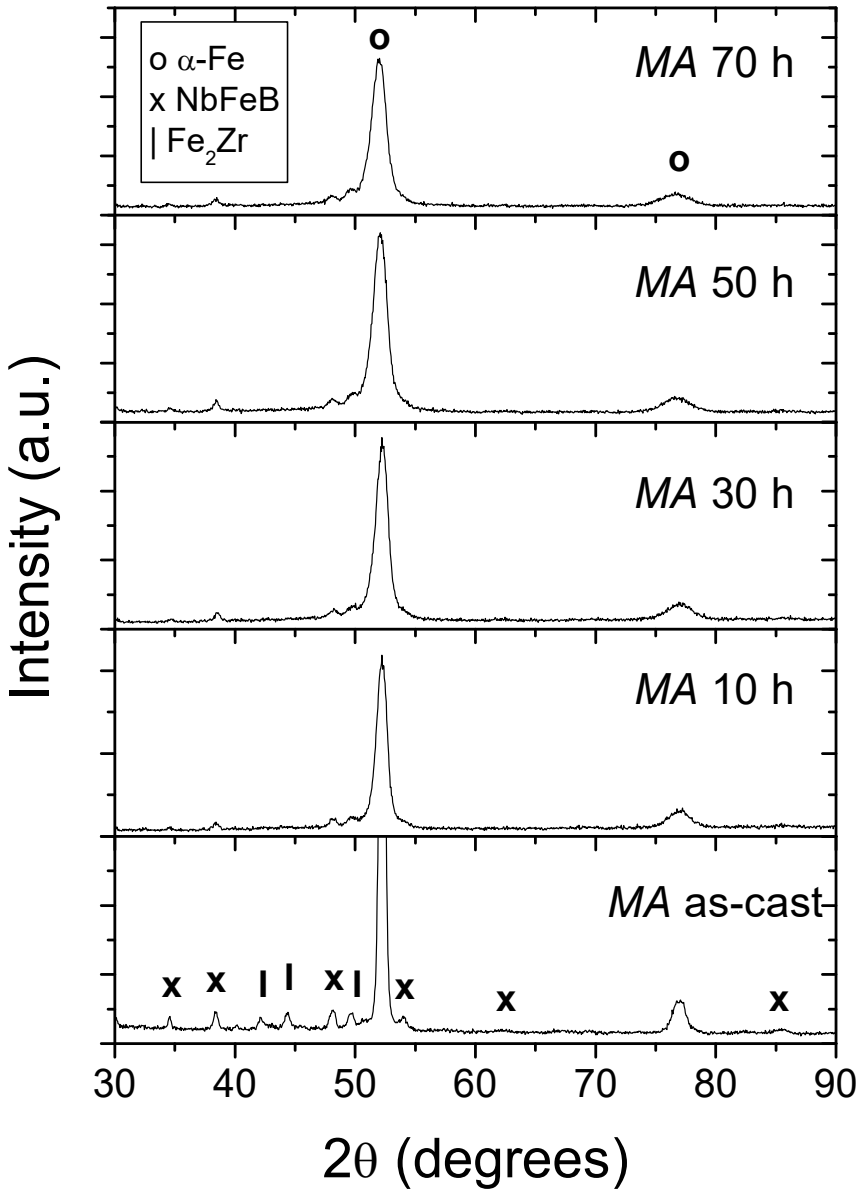

Philosophical Magazine. Vol. 86. Núm. 15. 2006. Pag. 2271-2282
http://dx.doi.org/10.1080/14786430500300074

Figure 4

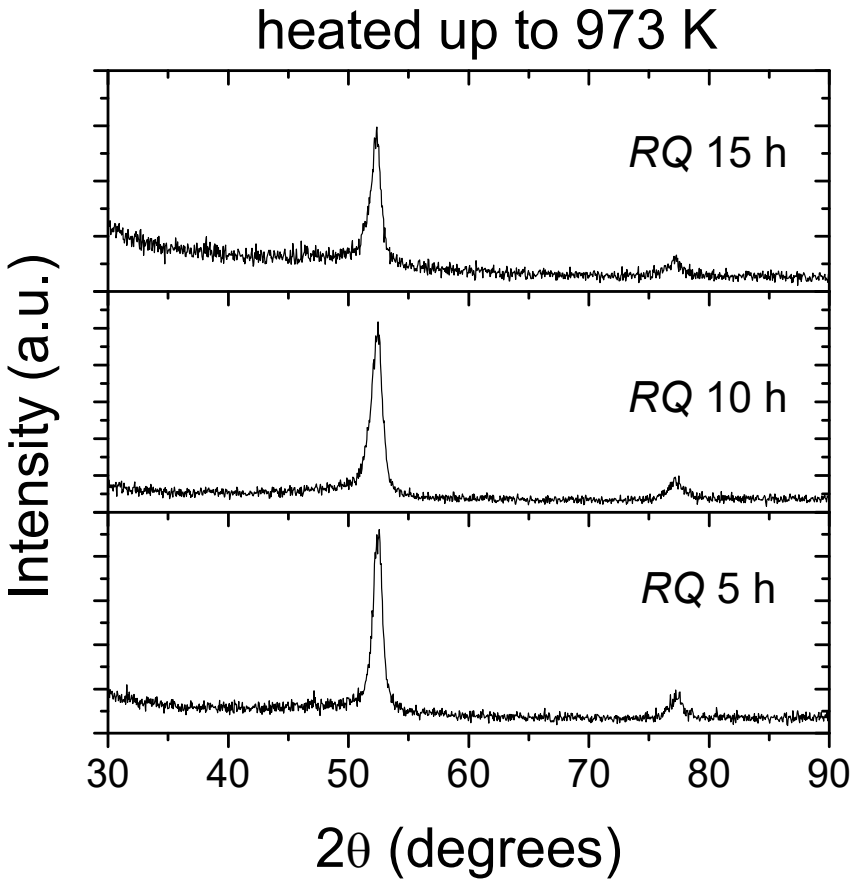

Philosophical Magazine. Vol. 86. Núm. 15. 2006. Pag. 2271-2282
http://dx.doi.org/10.1080/14786430500300074

Figure 5

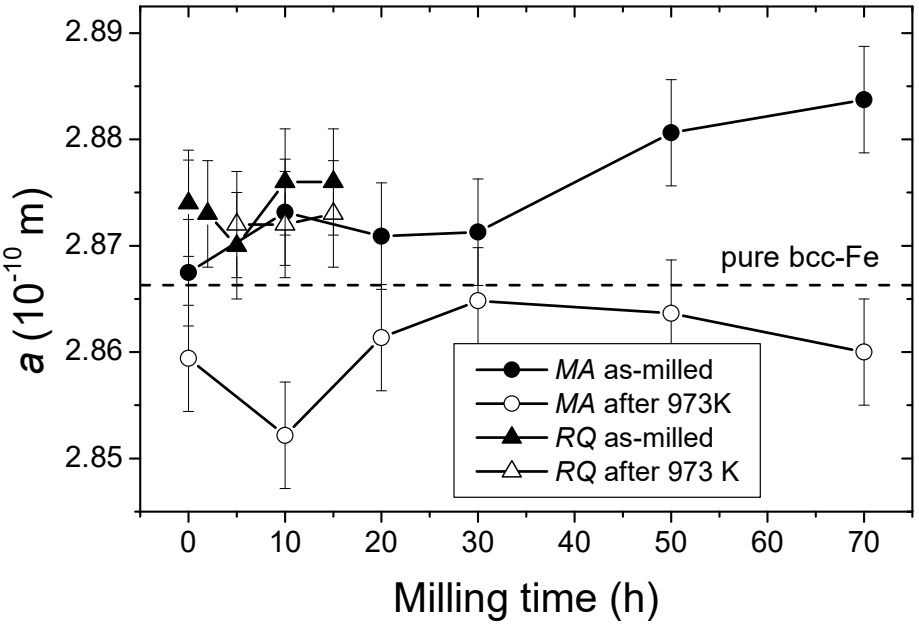

Philosophical Magazine. Vol. 86. Núm. 15. 2006. Pag. 2271-2282
http://dx.doi.org/10.1080/14786430500300074

Figure 6

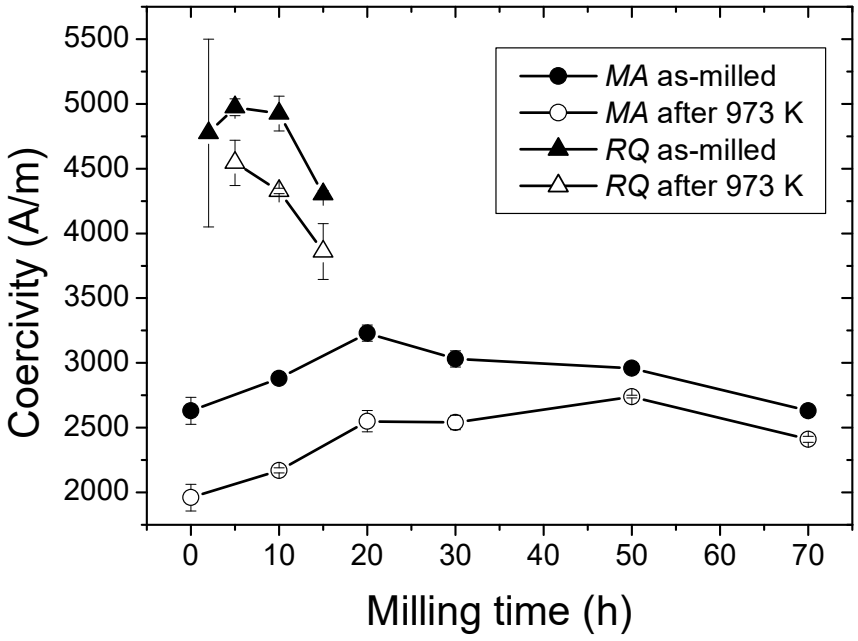

Philosophical Magazine. Vol. 86. Núm. 15. 2006. Pag. 2271-2282
http://dx.doi.org/10.1080/14786430500300074

Figure 7